EUROPEAN ORGANIZATION FOR NUCLEAR RESEARCH
CERN – ACCELERATORS AND TECHNOLOGY SECTOR

CERN-ATS-2011-024

New 2D Thermal Model Applied to an LHC Inner Triplet Quadrupole Magnet

E.R. Bielert[*+], G. Kirby[*], H.H. J Ten Kate[*+] and A.P.Verweij.[*]

[*]CERN, 1211 Geneva 23, Switzerland
[+]University of Twente, POB 217, 7500AE Enschede, The Netherlands

Abstract

A newly developed numerical model is presented that enables to compute two-dimensional heat transfer and temperature distributions over the cross-section of superconducting accelerator magnets. The entire thermal path from strand-in-cable to heat sink, including helium channels is considered. Superfluid helium properties are combined with temperature- and field-dependent non-linear solid material properties. Interfacial interactions are also taken into account. The model is applied to the cross-section of an inner triplet quadrupole magnet featuring a new concept for the ground insulation. Beam loss profiles are implemented as main heat source. It is concluded that operational margins can be considerably increased by opening additional thermal paths, improving the cooling conditions.

Presented at the International Cryogenic Engineering Conference 23–
International Cryogenic Conference 2010 (ICEC23–ICMC2010)
19-23 July 2010, Wrocław, Poland.

Geneva, Switzerland,
August 2011

INTRODUCTION

In the Large Hadron Collider at CERN, the final beam focus in the collider's interaction regions is provided by ―inner triplet‖ superconducting quadrupole magnets located at either side of the detectors. With the future luminosity upgrade of the LHC, the inner triplet will be replaced [1]. These magnets have to accept much higher levels of energy deposition by beam loss radiation than ever before. The main thermal design issue is the effective heat removal from the superconducting coil. Present magnets subjected to increased steady-state beam loss have a strongly reduced stability margin and are therefore more prone to quenching. Heat transfer must be drastically enhanced to guarantee a limited temperature rise and stable magnet operation. This asks for a new, improved design featuring optimized static and transient heat removal. Development of an advanced numerical model able to describe the thermal behavior of superconducting magnets in much more detail is needed. The model, once validated using existing experimental data, will be used as a tool to optimize the thermal design of new magnets, especially the inner triplet quadrupole upgrades using either Nb-Ti or Nb3Sn. Maximum heat removal is requested while satisfying mechanical and electromagnetic constraints [1]. Cable insulation and ground insulation layers are mandatory to avoid electrical shorts, but are also the main thermal resistances and thus primary for improvement. The focus here is to explain the new thermal model and to apply it to a new conceptual *ground* insulation, which can considerably enhance the heat removal.

NEW THERMAL MODEL

The model will be explained using the practical layout of an (MQXC) inner triplet quadrupole magnet as pictured in Figure 1, but is applicable to superconducting accelerator magnets in general. The entire thermal path from hot spot to heat sink in the cross-section of superconducting accelerator magnets is considered.The superconductors are located immediately around the beam pipe. Therefore the beam pipe —and after that the conductors— exhibit the highest volumetric heat load caused by beam loss. The windings are supported by a stainless steel collar, which is surrounded by an iron yoke. This structure is enclosed by a welded cylinder and filled with superfluid helium at 1.8 to 2.0 K and 1.3 bar. The yoke has four longitudinal holes, one containing a heat exchanger, which cools the magnet cold mass and shows a 0.2 K temperature gradient across the magnet length. Using 2D cross-sectional analyses, the heat exchanger is treated as a heat sink at the fixed worst case temperature of 2.0 K.

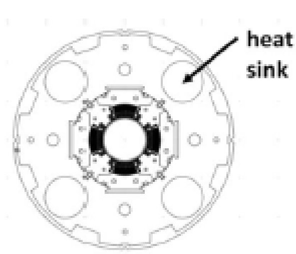

Figure 1 quadrupole magnet cross-section

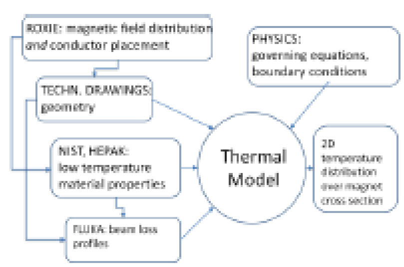

Figure 2 Schematic overview of thermal model

In the design of new magnets, beam pipe diameter and magnetic field (gradient) are fixed at an early stage. Next the position of the Rutherford type cables and shape of the iron yoke are specified (e.g. using the ROXIE code [2]) and used as an input for the thermal model. The magnetic field distribution over the magnet's cross-section is known and temperature – and magnetic field dependent material properties are implemented. Small changes in the geometry can be introduced to improve the thermal behavior, without interfering with the magnetic design. When thermal design requires more space, the magnetic design may be altered with an extra iteration. Convective heat transfer and black body radiation to the cold mass are not considered in this analysis. For inner triplet quadrupole magnets in nominal operation, steady-state energy deposition by beam loss and debris from collisions are the main heat sources. The amount and spatial distribution of beam loss are calculated using the FLUKA code [3]. To avoid three dimensional analyses, the by FLUKA given volumetric heat load is averaged over the length of the magnet. A worst case value of 45 Wm^{-1} over the complete cross-sectional surface is obtained. The beam pipe, with a relatively small total volume, has a heat load of 10 Wm^{-1}. The inner layer due to its larger total volume gets 13 Wm^{-1} and the outer layer 5 Wm^{-1}. Two dimensional analyses are justified since the magnet is long and the heat sources are simplified to be homogeneous along the magnet. Figure 2 shows schematically all the mentioned input for the thermal model. The thermal analyses are performed using the COMSOL multiphysics FEM code. With this code it is possible to implement the geometry, material properties and heat sources in a straightforward way. Conductive heat transfer is used as the governing equation to model the heat transport in the solid materials (see equation 1). Similar models applying the same equation using different codes already exist [4-10]. However modeling the entire thermal path in combination with the implementation of superfluid helium properties, solid material properties which are temperature and *magnetic field* dependent and the physical behavior at their interfaces in one overall model is new. The heat transport properties of superfluid helium are obtained from the Gorter-Mellink equation for turbulent heat transport in the two-fluid model (see equation 2) and implemented through an effective thermal conductivity [11]. This implies that the effective thermal conductivity, indicated by the term in brackets (see equation. 3a) is heat flux dependent. The numerical values for the superfluid helium heat conductivity function, *f(T)* at 1.3 bar are specified beforehand by the HEPAK code [12].

$$\nabla \cdot (-k(B,T)\nabla T) = Q(x,y) \quad , \tag{1}$$

$$\frac{\mathrm{d}T}{\mathrm{d}x} = -f(T)q^{m} \quad \text{, with } m\text{=3 as a theoretical value from the two fluid model,} \tag{2}$$

$$q = -\left(\left(\frac{1}{|f(T)|}\right)^{\frac{1}{m}}\left(\frac{1}{\left|\frac{\mathrm{d}T}{\mathrm{d}x}\right|}\right)^{1-\frac{1}{m}}\right)\frac{\mathrm{d}T}{\mathrm{d}x} \quad \text{, or as applied} \quad \vec{q} = -\left(\left(\frac{1}{|f(T)|}\right)^{\frac{1}{3}}\left(\frac{1}{|\nabla T|}\right)^{\frac{2}{3}}\right)\nabla T \quad , \tag{3a/b}$$

with *T*: temperature in K, *B*: magnetic induction in T, *Q*: volumetric heat load in Wm^{-3}, *k*: thermal conductivity in $Wm^{-1}K^{-1}$, $f(T)^{-1}$: superfluid helium heat conductivity function in $W^{3}m^{-5}K^{-1}$.

For interfaces between solids, negligible thermal contact resistance is assumed. For interfaces between kapton and superfluid helium, a Kapitza like resistance is used as in equation 4 [13], which is implemented as a thin resistive layer through equation 5:

$$R_K = (10540 \pm 444)T^{-3} \cdot 10^{-6} \quad , \tag{4}$$

$$-\boldsymbol{n}_u \cdot (-k_u \nabla T_u) = k_{res}(T_d - T_u)/d_{res} \quad \text{, making use of} \quad R_K = \frac{d_{res}}{k_{res}} \quad , \tag{5a/b}$$

with R_K : Kapitza resistance in Km^2W^{-1}, k_{res}: thermal conductivity in $Wm^{-1}K^{-1}$, d_{res}: layer thickness in m, $T_{d/u}$: temperature at interface (down/up) in K and $\boldsymbol{n}$: normal direction to the interface.
Some magnet thermal models [4, 9] are verified experimentally by correlating quench current to ramp rate loss heating or quench heater power. This is not a straightforward method as discussed by Verweij [14]. By calculating precise temperature fields with this new model it is possible to identify the bottlenecks in the thermal performance of magnets. When the temperature of the helium exceeds the lambda temperature, the thermal conductivity of helium suddenly drops orders of magnitude, stopping effective heat removal from the beam pipe and coil.

APPLICATION TO THE MQXC MAGNET

In previous models, relatively small heat loads are implemented. In this new model applied to the so-called MQXC magnet, beam loss heat loads due to the ultimate LHC luminosity are implemented. Calculations covering the total cross-section, including the iron yoke show that there is a negligible temperature drop of less than 1 mK across the yoke when the heat exchanger is fixed at 2.0 K, therefore the yoke is omitted in further analysis and the outer radius of the collar is set to 2.0 K. After this simplification the MQXC magnet has octant symmetry, therefore the FEM model covers only one eighth of the total cross-section of the magnet (Figure 3).

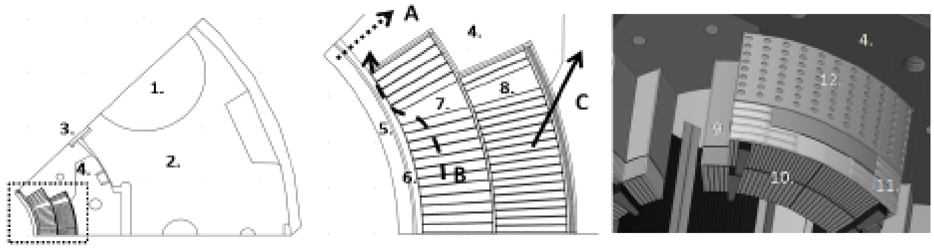

1. Heat exchanger (sink)
2. Iron yoke
3. Key
4. Stainless steel collar
5. Beam pipe and insulation
6. Helium annulus
7. Inner layer coil + Cu wedge
8. Outer layer coil + Cu wedge
9. Ground insulation
10. Quench heaters
11. Fishbone
12. Protection sheet

Figure 3 (left) quadrupole octant, (middle) zoom of the coil, (right) 3D representation

The magnet has a 120 mm bore and a two layer design. It is made of standard LHC Nb-Ti Rutherford cables, insulated with enhanced cable insulation [15]. The packing factor is chosen such that the helium between the yoke laminations fills 6% of the total volume, enough to allow superfluid helium to easily transfer heat to the sink [6]. Because of the laminations an inhomogeneous thermal path in longitudinal direction is obtained. The collar and yoke laminations and the helium in between are modelled as parallel thermal resistances in radial direction. With all the material properties and the packing factors known, average material properties are calculated and implemented by the volumetric ratio between steel and superfluid helium. In the center plot of Figure 3, three different thermal paths to the heat sink are indicated: A, from the beam pipe; B, from the inner layer and C, from the outer layer. Figure 4 shows schematically the thermal resistances for each path, wider blocks representing larger resistances (not scaled). It shows that cable insulation and ground insulation are of major interest. Also the flap of the ground insulation reaching out into the helium annulus (space between coil and beam pipe) and blocking the heat flux to the sink is of great importance. Much effort has been made in improving helium transparency of the cable insulation.

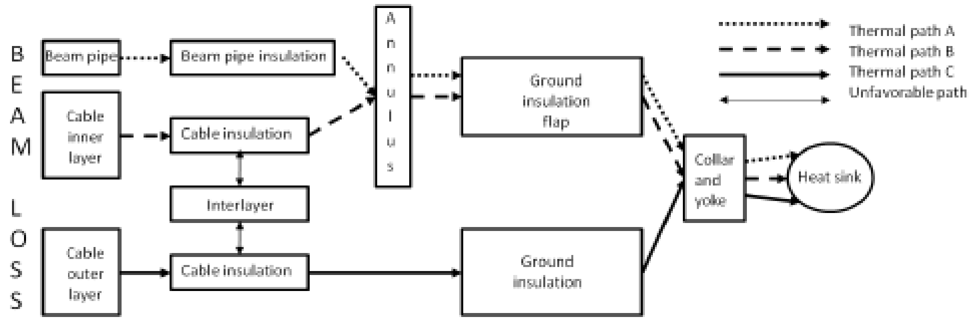

Figure 4 Thermal paths from heat source to heat sink

As is clear from Figure 4, the superconductors in the inner layer are cooled through the cable insulation by the helium annulus and further radially outward to the heat sink through the superfluid helium in between the collar and yoke laminations. The beam pipe is cooled in a similar way as the inner layer. In the old LHC design, the heat flow from the outer layer to the heat exchanger is through the cable insulation and by conduction through the four layers of kapton ground insulation (0.5 mm total thickness) and the stainless steel protection sheet. The new concept of ground insulation results in better cooling of the outer layer by introducing open helium channels (Figure 3 right plot). The four layers of kapton ground insulation normally sealing the coil from the collar are now opened, but are still overlapping such that the integrity of the electrical insulation is maintained (Figure 5). In between the kapton layers (grey) and the coil (dark grey), an extra layer that includes helium channels, called fishbone, is placed (white). The stainless steel protection sheet (black) is also made transparent for helium by introducing holes, making it 30% open. It allows heat from the outer layer of the coil to flow radially outward. In between the two coil layers, a newly designed quench heater is introduced (Figure 6). It has a wavy shape such that all conductors are still covered and has holes which allow helium to penetrate easily.

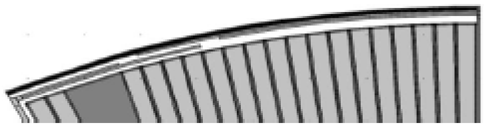

Figure 5 Open ground insulation of second layer

Figure 6 Quench heater with cooling holes

Temperature distributions for the standard and open ground insulation show that the peak temperature in the inner layer is reduced from 3.16 K to 2.56 K by implementing the modified open ground insulation. The position of the peak temperature moves from the inner layer to the beam pipe. In addition, the influence of kapton ground insulation reaching into the annulus is analyzed. Its effects are annulus blockage and poorer cooling of the inner layer and beam pipe.

Only with the new ground insulation the outer layer is cooled well. Figure 7 shows temperature profiles for these four cases and Table 1 summarizes the peak temperatures found in beam pipe, inner layer and outer layer. An interesting fact is that at zero beam loss the smallest temperature margin can be found at the most outer conductor. The absolute temperature distribution shows that the smallest temperature margin is located at the midplane conductor. Using the critical surface of Nb-Ti (taking into consideration the magnetic field *and* temperature), it is shown that the smallest temperature margin can be located at a conductor anywhere in between the midplane and outer conductor, depending on the exact field – and temperature distribution.

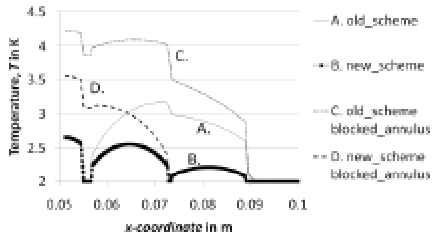

Figure 7 Temperature profile through the middle of the midplane conductors radially outward

Table 1 Peak temperatures

	Old scheme	New scheme
Unblocked annulus	Beam pipe 2.66 K Inner layer 3.16 K Outer layer 2.97 K	Beam pipe 2.66 K Inner layer 2.56 K Outer layer 2.22 K
Blocked annulus	Beam pipe 4.22 K Inner layer 4.10 K Outer layer 3.48 K	Beam pipe 3.55 K Inner layer 3.12 K Outer layer 2.22 K

CONCLUSION

The newly developed numerical model runs stably and application to the new concept for the ground insulation shows that the temperature margin for a typical quadrupole magnet can be significantly increased. Introducing new helium channels spreads out the heat flux. A lower heat flux density in the annulus results in a higher thermal conductivity of the superfluid helium. The inner layer and beam pipe are thus also better cooled when the ground insulation is open. Removing the flaps of ground insulation can create a more open annulus. These interesting results ask for experimental validation, which will be provided in the near future. The model will be extended step-by-step to be able to describe the magnet's thermal behavior across the entire operational temperature range of 1.9 to 10 K, including transient calculations, phase transition to liquid helium and cooling by natural convection of liquid helium. Also phase transition of the superconductor to the normal phase accompanied by Joule heating will be covered.

REFERENCES

1. Ostojic, R., *et.al.*, Conceptual design of the LHC interaction region upgrade – phase I, LHC Project Report 1163 (2008)

2. Russenschuck, S., ROXIE – a computer code for the integrated design of accelerator magnets, Proc. EPAC-98, (1999)

3. Hoa, C. And Mokhov, N.V. and Cerutti, F. And Ferrari, A., Inter-comparison of MARS and FLUKA: predictions on energy deposition in LHC IR quadrupoles, LHC Project Note 411 (2008)

4. Bocian, D., Dehning, B., Siemko, A., Modeling of quench limit for steady state heat deposits in LHC magnets, IEEE Trans. Appl. Supercond. (2008) 18-2 112-115

5. Yadav, S., Zlobin, A., Finite Element Analysis of the effect of cooling conditions on two-layer and four-layer HGQ magnet designs, Fermilab Technical Note TD-02-047 (2002)

6. Huang, Y., Kerby, J., Mazur, P.O., Peterson, T.J., Zlobin, A., Thermal design of a high gradient quadrupole for the LHC interaction regions, IEEE Trans. Appl. Supercond. (1997) 7-2 578-581

7. Novitski, I., Zlobin, A., Thermal analysis of SC quadrupoles in accelerator interaction regions, IEEE Trans. Appl. Supercond., (2007) 17-2 1059-1062

8. Kashikhin, V.V., Bossert, R., Chlachidze, G., Lamm, M., Mokhov, N.V., Novitski, I., Zlobin, A.V. Performance of Nb3Sn quadrupole magnets under localized thermal load, Adv. Cryog. Eng.: Trans. CEC 2009 (2010) 55 499-506

9. Chiesa, L., *et al*., Thermal studies of a high gradient quadrupole magnet cooled with pressurized, stagnant superfluid, IEEE Trans. Appl. Supercond., (2001) 11-1 1625-1628

10. Drozhdin, A.I.,*et al*., Radiation and thermal analysis of superconducting quadrupoles in the interaction region of linear collider*, Proc. of EPAC08, Genova, Italy (2008)

11. Van Sciver, S.W., Helium Cryogenics, Plenum Press, New York, USA (1986) 166-182

12. Cryodata Inc., User's Guide to HEPAK, Version 3.4, Louisville, Colorado, USA (1999)

13. Baudouy, B., Kapitza resistance and thermal conductivity of Kapton in superfluid helium, Cryogenics, (2003) 43 667-672

14. Verweij, A.P., Electrodynamics of superconducting cables in accelerator magnets, PhD thesis, University of Twente, Enschede, The Netherlands (1995) 193-222

15. Granieri, P.P., *et al*., Heat transfer in an enhanced cable insulation scheme for the superconducting magnets of the LHC luminosity upgrade, IEEE Trans. Appl. Supercond. (2010) 20-3 168-171